.

CHEMICAL OZONE LOSS AND RELATED PROCESSES IN THE ANTARCTIC WINTER 2003 BASED ON ILAS-II OBSERVATIONS

Simone Tilmes[1,3], Rolf Müller[1], Jens-Uwe Grooß[1], Reinhold Spang[1], Takafumi Sugita[2], Hideaki Nakajima[2], Yasuhiro Sasano[2]

[1]Institute of Stratospheric Research (ICG-I), Jülich, Germany

[2]Atmospheric Environment Division, National Institute for Environmental Studies, Japan

[3]currently at National Center of Atmospheric Research, Boulder, CO, USA

Short title: CHEMICAL OZONE LOSS IN THE ANTARCTIC WINTER 2003

Abstract. In this study, ILAS-II (Improved Limb Atmospheric Spectrometer) measurements were used to analyze chemical ozone loss during the entire Antarctic winter 2003, using the tracer-tracer correlation technique. The temporal evolution of both the accumulated local chemical ozone loss and the loss in column ozone in the lower stratosphere is in step with increasing solar illumination. Half of the entire loss in column ozone of 157 DU occurred during September 2003. By the end of September 2003, almost the total amount of ozone was destroyed between 380 and 470 K. Further, ozone loss rates were strongly increasing during September for the entire lower stratosphere. The values of accumulated ozone loss and ozone loss rates strongly depend on the altitude. During September, ozone mixing ratios show a large day to day variation. Box model simulations by the Chemical Lagrangian Model of the Stratosphere (CLaMS) show that this is a result of the different history of the observed air masses. Further, the box model supports the general evolution of ozone loss values during September as a result of strong increase of halogen catalyzed ozone destruction.

1. Introduction

Chemical ozone loss in the lower polar stratosphere has been a research focus since the discovery of the Antarctic ozone hole in the mid-eighties [*Farman et al.*, 1985]. Severe chemical ozone destruction during the winter period in the Antarctic and, in recent cold winters, also in the Arctic is a result of anthropogenic emissions of long-lived halogen compounds (in particular CFCs and halons) to the atmosphere. Chlorine reservoir species (in particular HCl and $ClONO_2$) are activated mainly on the surface of polar stratospheric clouds (PSCs) that exist in a sufficiently cold winter polar stratosphere. The resulting photo-labile forms of chlorine are photolyzed upon exposure to sunlight. In spring, even at low sun, effective ozone destroying catalytic cycles [*Molina and Molina*, 1987; *McElroy et al.*, 1986; *Solomon et al.*, 1986] cause significant ozone loss.

During the past decade, the analysis of ozone loss and related processed in the stratosphere in polar regions has mainly focused on the Arctic [e.g., *Müller et al.*, 1999; *Rex et al.*, 2004; *Goutail et al.*, 2003; *Manney et al.*, 2003; *Tilmes et al.*, 2003, 2004; *Harris et al.*, 2003, and references therein]. Various methods were used to derive chemical ozone loss and chlorine activation and their relation to meteorological conditions [e.g., *Rex et al.*, 2002; *Harris et al.*, 2002; *Tilmes et al.*, 2004]. Further, various model studies were performed to investigate Arctic and Antarctic winter ozone loss. Especially the Arctic early winter chemical ozone loss and the ozone loss above the 475 K potential temperature level was underestimated by models [e.g., *Becker et al.*, 1998, 2000; *Rex et al.*, 2003]. Discrepancies between model and measurements still exist, although recent studies indicate that models are able to reproduce Arctic ozone loss [*Chipperfield et al.*, 2005]. Further, *Brasseur et al.* [1997] reported that their model does reproduce the Antarctic total column ozone depletion as observed by TOMS.

In that study by *Brasseur et al.* [1997], the maximum of observed total ozone depletion over the Antarctic is in agreement with satellite measurement. However, besides continuous total column ozone measurements (e.g., by TOMS),

no continuous data set of mixing ratios of different species, as ozone, were available over an entire Antarctic winter, to compare model results.

Using measurements of O_3 and N_2O by the ILAS-II instrument aboard the ADEOS-II satellite, it is possible for the first time, to estimate chemical ozone loss continuously over an entire Antarctic winter using tracer-tracer correlations. The temporal development of local accumulated ozone loss will be analyzed, as well as the accumulated loss in column ozone. A comparison with meteorological conditions will be conducted using UK meteorological analysis for different altitude ranges.

The continuous ILAS-II data set further allows deriving ozone loss rates per day within the polar vortex at different altitude intervals. These values can be compared to the ozone loss rates that will be deduced from the results of the first Match ozone sonde campaign in the Antarctic that was conducted during winter 2003 (P. v. d. Gathen, pers. comm.). Additionally, the ILAS-II observations during September, 2003, will be compared with results of a box model simulation of the Chemical Lagrangian Model of the Stratosphere (CLaMS) [*McKenna et al.*, 2002b, a], to scrutinize the large ozone loss values derived for September, 2003.

2. ILAS-II Measurements and Method

The ILAS-II (Improved Limb Atmospheric Spectrometer) instrument aboard ADEOS-II (Advanced Earth Observing Satellite) observed the entire Antarctic winter 2003 continuously from April 2 to October 24, 2003 [*Nakajima et al.*, 2005]. The occultation satellite instrument is measuring sunrise and sunset data up to 14 times per day. The sunset mode of the instrument covers the area of the polar vortex very well during the entire austral winter and spring (Figure 1) and is therefore well suited to observe chemical ozone loss. Poleward of the latitude of the measurement location (Figure 1, gray area) the earth was not illuminated between April and mid-September.

Figure 1.

The ILAS-II Version 1.4 data set (the first public release) includes O3, HNO3,

N2O, CH4, and aerosol extinction coefficient at 780 nm data from cloud top up to 70 km. Vertical profiles of other atmospheric trace gases such as NO2, H2O, ClONO2 and N_2O5, were also retrieved during the entire measurement period (not validated yet).

In this study, the tracer-tracer correlation method [e.g., *Proffitt et al.*, 1990; *Müller et al.*, 2001; *Tilmes et al.*, 2003, 2004] is used to calculate chemical ozone loss. Using this method, deviations from an early winter reference function derived for chemically unperturbed conditions in an established vortex are used to identify chemical ozone loss. Here, N_2O can be used as the long-lived tracer. Although there is an offset of N_2O ILAS-II Version 1.4 data compared to ODIN/SMR (v1.2) (Sub-Millimeter-Radiomenter) for N_2O mixing ratios less than 100 ppbv, this offset does not show any seasonal change [*Ejiri et al.*, 2005; *Urban et al.*, 2005]. A constant offset of the long-lived tracer used will not affect the results of tracer-tracer correlation analysis.

3. Meteorology of the Antarctic Winter 2003

Figure 2.

The Antarctic vortex started forming during March 2003 [*Tilmes et al.*, 2005b], at the time when an edge of the vortex started to exist using the algorithm by [*Nash et al.*, 1996]. During the setup phase of the vortex, two relative maxima of the gradient of potential vorticity exist using UK meteorological analysis. The vortex was partly separated in two regions, one region was located within equivalent latitudes equatorward of 70°S and another within the region poleward of 70°S equivalent latitude (inner vortex) [*Tilmes et al.*, 2005b]. On the basis of that study, the polar vortex edge was calculated for these two separate regions as well. During April to October 2003, a continuous polar vortex edge could be determined equatorward of 70°S at altitudes between the 475 and 650 K potential temperature level (Figure 2). The potential vorticity at the edge of the vortex is increasing until mid-July (Figure 2, solid lines). An indication of a disturbance of the vortex is noticeable during the second part of July, because the potential temperature of the

edge of the vortex significantly decreases at 650 K. However, at altitudes below 650 K the potential vorticity at the edge of the vortex is still increasing until October, 2003, and no minor warming was observed in this winter [pers. comm. M. Streibel]. Additionally to the vortex edge, an inner vortex edge was determined poleward of 70°S, for certain time intervals. An inner edge was found for the setup phase of the vortex [*Tilmes et al.*, 2005b], at the time of a slightly disturbed vortex in July and at the end of September and in October, 2003, at altitudes of 650 K. During November, only an inner vortex edge could be determined using the *Nash et al.* [1996] criterion at altitudes above 550 K. At this time the vortex is breaking down although vortex remnants continue to exists until the end of November.

Figure 3.

The area of possible PSC existence (A_{PSC}) deduced from analyzed stratospheric temperatures and sun light hours per day have an influence on chemical ozone loss within the lower stratosphere [*Tilmes et al.*, 2004]. In this study, we will use these values for the interpretation of chemical ozone loss values.

The PSC threshold temperature was calculated with averaged mixing ratios of ILAS-II HNO_3 and H_2O measurements. Using a HNO_3 mixing ratio of 10 ppbv and a H_2O mixing ratio of 5 ppmv, as it is done for Arctic conditions [*Tilmes et al.*, 2005a], A_{PSC} is a factor 0,28 larger than deduced using ILAS-II measurements. Thus the decrease of HNO_3 and H_2O mixing ratios, cause by the impact of denitrification and dehydration, on the threshold temperature for PSCs should be included in the calculation of A_{PSC} for Antarctic conditions.

Additionally, in the Antarctic winter 2003, measurement of daily mean PSC cloud top heights of the Michelson Interferometer for Passive Atmospheric Sounding (MIPAS) aboard ENVISAT [*Spang et al.*, 2005] are available (Figure 3, black plus signs). Additional to A_{PSC}, these measurements are a precise information about PSC occurrence.

Calculated A_{PSC} and actually detected mean PSC cloud top heights by MIPAS are in general agreement. Stratospheric temperatures reached the threshold for PSC existence since mid-May until the end of September 2003 (Figure 3). First

Sulfuric Ternary Solutions (STS) particles were measured at the end of May by MIPAS and first Nitric Acid Trihydrate (NAT) particles in June 10–12, 2003 at altitudes below 24 km ($\approx$ 650 K). Since July 20, mean cloud top hight detected by MIPAS are below 580 K. With the descent of the vortex air masses, mean PSC cloud top heights are significantly decreasing from 570 K to 400 K during August. During the entire September 2003, a A_{PSC} was calculated at altitudes below 500 K and MIPAS mean cloud top heights of PSC are below 470 K.

4. Tracer-tracer Correlations

Figure 4.

Chemical ozone loss in the polar vortex can be derived from satellite measurements in using the tracer-tracer correlation technique [e.g., *Proffitt et al.*, 1990; *Müller et al.*, 1996; *Tilmes et al.*, 2004]. Using this technique, an early winter reference function for the ozone-tracer relation in the established polar vortex is derived. Deviations from this reference function can be attributed to chemical ozone loss, because transport processes can be excluded using tracer-tracer correlations within an isolated vortex [*Müller et al.*, 2001; *Tilmes et al.*, 2003, 2004; *Müller et al.*, 2005].

The evolution of the incipient Antarctic polar vortex between March and June 2003 is discussed in detail in *Tilmes et al.* [2005b]. In that study it is shown that tracer-tracer correlations throughout the entire vortex are compact and constant by mid-June, 2003, and that the vortex core is isolated at that time. At this time of the year, during the polar night, no chemical ozone loss is expected to occur. Therefore, a reference for chemically unperturbed conditions is derived for in June 11–20, 2003 from ILAS-II measurements that are located in the Antarctic polar vortex core (see Figure 4, panel a, black line).

Although, ILAS-II profiles are located at rather low geographical latitudes up to 65°S (see Figure 1), the equivalent latitudes of these measurements range between 65 and 90 °S (see Figure 4, panel a). This is the case because the vortex core is not steadily located above the geographic South pole but is sometimes

shifted towards lower geographical latitudes. All these profiles are used to derive the early winter reference function.

To allow a precise comparison of ILAS-II measurements with the synoptic meteorological data, the position of ILAS-II profiles are converted to noon time using trajectory calculations based on UKMO wind data [*Tilmes et al.*, 2003].

Using N_2O as a long-lived tracer (mixing ratios in ppbv) and O_3 (mixing ratios in ppmv) the early winter reference function (valid for range 10 ppbv $< N_2O <$ 300 ppbv) is derived as:

$$\begin{aligned} O_3 &= 1.81 \cdot 10^{-9} \cdot (N_2O)^4 - 8.40 \cdot 10^{-7} \cdot (N_2O)^3 + 6.43 \cdot 10^{-5} \cdot (N_2O)^2 \\ &\quad -1.72 \cdot 10^{-3} \cdot (N_2O) + 3.12 \end{aligned} \quad (1)$$

The scatter of profiles inside the polar vortex measured by the standard deviation is estimated to be $\sigma = 0.2$ ppmv.

Ozone mixing ratios of profiles located poleward of an equivalent latitude of 80°S scatter up to 0.5 ppmv below the derived reference function for altitudes above the 100 ppbv N_2O level (Figure 4, panel a, green profiles) possibly as a result of a slight isolation between a previously existing inner vortex within the entire vortex. An overestimation of chemical ozone loss of profiles located poleward of an equivalent latitude of 80°Sis therefore possible, but included within the range of uncertainty. of the reference function. Note however that the air mass poleward of 80°S constitutes only about 25% of the air mass poleward of 70°S.

By mid-July 2003, significant deviations from the early winter reference function occur (not shown) and at the beginning of August all profiles measured inside the vortex core scatter below the early winter reference function (Figure 4, panel b); including profiles located poleward of equivalent latitude of 80°S.

During August and September, the signature of chemical ozone loss in the evolution of tracer-tracer profiles is becoming clearly noticeable (Figure 4, panel b to g). During August, the strongest deviations from the reference occur for profiles located towards lower equivalent latitudes, between 70°S and 80°S (red and blue profiles). This is because these profiles are influenced by a larger amount

of sunlight that enhances ozone destruction. During September 20–30, rather suddenly, all profiles inside the polar vortex core indicate a very strong decrease of ozone mixing ratios towards zero (see Figure 4, panel g). The temporal evolution of ozone loss during the second part of September will be discussed in detail below in Section 5.2. During October 2003, very low ozone mixing ratios were reached – between 0.0 and 0.4 ppmv between the 80–240 ppbv N_2O level – for all profiles measured inside the Antarctic polar vortex.

5. Accumulated Ozone Loss

The accumulated local ozone loss is ozone loss that occurred in the period between the time of the early winter reference function and the date considered to derive the ozone loss. Ozone loss is derived over an altitude interval between 350 and 600 K potential temperature. For interpretation of a large scatter of ozone loss profiles, daily variations of ozone mixing ratios will discussed as well. Additionally, we show the temporal evolution of local ozone loss averaged within certain altitude ranges, smoothed over 10 days. The results will be discussed and compared with meteorological analyses. Further, the temporal evolution of loss in column ozone derived between 350 and 600 K will be shown.

5.1. Local Ozone Loss Profiles

Figure 5.

The temporal evolution of accumulated local ozone loss profiles can be followed during the entire Antarctic winter 2003 using ILAS-II measurements. In Figure 5, vertical ozone profiles measured within the vortex core (red lines) and estimated ozone loss profiles (black lines) are shown for a period of ten days in each panel to give an overview.

The early winter reference function was derived for June 11–20, 2003. At this time, the ozone loss profiles do not show any ozone loss, as expected. Solely, two profiles that are located poleward of the equivalent latitude of 80°S show an ozone loss (ΔO_3) of $\approx$ 0.5 ppmv for altitudes above about 500 K. As described in

Section 4, this observation should not be attributed to chemical ozone loss.

Beginning in August, significant local ozone loss occurred (Figure 5, black lines), at altitudes between 350 and 600 K potential temperature. At the end of August, the average of local ozone loss between 400 and 550 K is 0.79 ppmv with a standard deviation of 0.31 ppmv. During mid-August, a maximum of accumulated ozone loss of 1.5 ppmv occurred at altitudes between 460 and 520 K potential temperature.

During September, ozone loss profiles show a much stronger scatter compared to August, 2003. The standard deviation of local ozone loss profiles in the first half of September reaches 0.37 ppmv. In the second half of September, loss profiles scatter less, however, inside the vortex core a separation of ozone loss profiles is obvious between 400 and 500 K during September 21–30, 2003 (Figure 5). On the one hand, maximum ozone loss values less than $\approx$ 2.3 ppmv were measured before March 25, and, on the other hand maximum local ozone loss larger than 2.3 ppmv was measured after March 25. We will discuss this in detail in Section 5.2. The averaged local ozone loss between 400 and 550 K is 2.3 ppmv. At the end of September, a maximum local ozone loss of 2.8 ppmv was reached at $\approx$ 475 K potential temperature with an average of 2.5 between 400 and 550 K.. Since the beginning of October, chemical local ozone loss is very homogeneous for all profiles measured by ILAS-II and the maximum and averaged local ozone loss has not increased after the end of September, however the standard deviation has decreased towards 0.08 ppmv. Ozone mixing ratios were not decreasing any more during October.

5.2. Daily Variations of Ozone Mixing Ratios

Figure 6.

In this section, the strong variability of vertical ozone loss profiles during September (Figure 5) will be discussed. Figure 6, bottom panel, shows the ozone mixing ratios for two potential temperature levels, at 500 K and 550 K, between September 5–10, observed within the vortex core. Strong daily variations of ozone mixing ratios of about 1 ppmv are obvious that cannot be explained by differences

in equivalent latitude. To investigate this findings in more detail, backward trajectory calculations were performed starting at the observations.

Some of the 20 day back trajectories of observed air masses did stay close to the pole while others originated from low latitudes. Figure 6, top panel, shows the fraction of time at which each air parcel has been in sunlight (solar zenith angle $< 95°$). The sunlight fraction of the back trajectory of the observations is varying between 8% and 45%. Indeed it is obvious that air masses with high sunlight fraction – that obtained more sunlight – correspond to the observations of low ozone mixing ratios and vice versa.

Further, the amount of illumination controls the amount of $ClONO_2$ mixing ratio. If large ClO mixing ratios prevail, the ClONO2 production is controlled by the production of NO_2 from photolysis (and reaction with OH) of HNO_3. $ClONO_2$ mixing ratios were larger if the observed air mass was illuminated more strong during 20 days before the measurements time (not shown). As long as some amount of chlorine is still activated, larger $ClONO_2$ correspond to smaller ozone mixing ratios occurring for larger illumination. Therefore, at this time of the year, the large variation of ozone mixing ratios and ozone loss values is a result of the different history of observed air masses.

Figure 7.

Until in September 24, 2003, the variability of sunlight time fraction of backward trajectories has decreased (Figure 7, top panel), since all vortex air was exposed to a significant amount of sunlight. In correspondence, the variability of ozone mixing ratios and therefore the variability of ozone loss values is decreasing as well.

Back-trajectory analysis further indicate that between September 24–26, the characteristics of airmass history have changed. The latitude over the last 20 days of the observed air parcels at 500 K potential temperature has changed from 85°S ± 3 °S at September 24, to 75°S ± 4.°S at September 26 (Figure 7). Therefore, airmasses observed before September 24 and after September 26 are not necessary comparable and the day-to-day variations in ozone should not be interpreted as

chemical change between September 24 and 26, 2003. Further, larger variations in sunlight time between September 24–26 is becoming obvious compared to some days before (Figure 7). However, at this time, the air masses indicating the lowest ozone mixing ratios received the smallest number of sunlight hours during 20 day before the measurement. This is in contrast to the anti correlation between ozone mixing ratios and sunlight time that was found during the first part of September. In late September, the stronger illumination of air masses has possibly resulted in an almost complete chlorine deactivation and therefore less ozone loss values.

From September 26 on, the history of air masses has changed compared to September 24 (Figure 7). Ozone mixing ratios are rather homogeneous and are slightly increasing with decreasing averaged latitudes for 20 day backward trajectories and increasing solar illumination between September 26 and 30.

To remove the effect of the explained short term variability in ozone mixing ratios and therefore local ozone loss values, in the following analysis local ozone loss will be smoothed. However, during September 24–27 (depending on altitude) local ozone loss values and deduced ozone loss rates may be still influenced by the observations of not comparable air masses.

5.3. General Evolution of Local Ozone Loss

Figure 8.

To describe the general temporal evolution of local ozone loss, the daily averaged ozone loss values in the vortex core smoothed over a period of 10 days. This was likewise done for meteorological values as the solar illumination on the area of PSC existence (A_{PSC}) and the possible area of PSC existence (A_{PSC}). Four different altitude ranges, 380–420 K, 430–470 K, 520–560 K, and 580–620 K, are considered separately (Figure 8).

Chemical ozone loss started in July 2003 for all altitudes considered with beginning illumination, in accordance with the current understanding of ozone destruction. Further, chemical ozone loss is expected to correlate with A_{PSC}. The largest A_{PSC} was calculated for 380-420 K and 420–470 K and in correspondence, the largest ozone loss occurred in these altitude regions. Ozone loss of 1.2 $\pm$ 0.2

ppmv was calculated until the beginning of September 2003 for these two altitude intervals. Until September 22–23, 2003, the ozone loss reached 2.3 ± 0.2 ppmv below 470 K potential temperature and ozone mixing ratios were below 0.3 ppmv. After this date, the remaining ozone was almost completely destroyed until the beginning of October, 2003 (Figure 8, top panel, red line). At altitudes of 430–470 K, ozone loss increased until the beginning of October up to 2.8 ± 0.2 ppmv until ozone mixing ratios were nearly zero. Thus, almost the total amount of ozone between 380 K and 470 K was destroyed until the end of September.

For altitude intervals 520–560 K and above, accumulated ozone loss is less, possible because the A_{PSC} is decreasing from July on. Further, mean PSC cloud top height detected by MIPAS is strongly decreasing during August (Section 3). Since mid-September, the PSC probability is nearly zero derived using UKMO analysis at these altitudes and no PSC events were detected by MIPAS during the entire September. Until September 1, 2003, 0.8 ± 0.2 ppmv ozone loss was reached in 520–560 K. During the second part of September, 2003, a strong increase of accumulated ozone loss occurred, up to 1.9 ± 0.2 ppmv until the beginning of October, 2003. This increase is the largest compared to altitudes below. In those altitudes ozone loss is not limited by the prevailing ozone mixing ratios as it is the case at lower altitudes (see Figure 8, red lines). Further, the ozone loss is enhanced by enhanced solar illumination during this time of the year (see Section 7, for further discussion). However, as described in Section 5.2, the increase of accumulated ozone loss is possibly enhanced by the changing air masses observed during the second half of September, therefore, estimated ozone loss rates (Section 6) are possibly overestimated.

At 580–620 K, a large A_{PSC} was derived using UK meteorological analysis and, further, PSCs were measured by MIPAS until mid-July, 2003 (Figure 2). At these altitudes, accumulated ozone loss is almost zero (within the range of uncertainty) until September, 2003. Only during September some ozone loss occurred that increases up to 0.4 ± 0.2 ppmv at the beginning of October 2003.

5.4. Accumulated Ozone Loss in column ozone

Accumulated chemical ozone loss in column ozone is derived by integrating the ozone loss profiles over a certain altitude range [e.g., *Tilmes et al.*, 2004; *Salawitch et al.*, 2002]. Here, the altitude range of 350 and 600 K potential temperature is used, the altitude range over which the halogen catalysed polar ozone loss occurs (as discussed above). The temporal evolution of chemical loss of column ozone inside the vortex core is shown in Figure 9. Accumulated ozone loss is smoothed here over 20 days to eliminate any short term variability.

Figure 9.

In addition to ozone loss (black line), the area of possible PSC existence is shown (blue line), averaged over the same altitude range (350–600 K). First STSs were detected by MIPAS already in mid-May. The volume of possible PSC existence increases up to its maximum at the beginning of August and is decreasing thereafter. Solar illumination at PSC area increases since the beginning of July. Only with increasing solar illumination, chemical ozone loss started in July 2003 as expected from the current understanding of polar ozone destruction mechanisms. At the beginning of September 2003, 79 ± 17 DU ozone were destroyed. This is half of the entire ozone loss of 157 ± 17 DU that occurred until the beginning of October 2003. In step with increasing sun hours per day, ozone loss is increasing during the entire winter until October. About 88% of the proxy ozone (ozone for chemically unperturbed conditions) is destroyed in 350–600 K at the beginning of October. As discussed in Section 5.3, the most effective ozone destruction occurred at altitudes below 470 K.

Loss in column ozone calculated over the altitude range of 380–550 K (115 ± 15 DU) can be compared with ozone loss that was derived for very cold Arctic winters. For example, in the cold winter 1999-2000 with a vortex located close to the pole, column ozone loss of 83 ± 6 DU inside the vortex core were derived using HF as a long-lived tracer [*Tilmes et al.*, 2004]. Another cold Arctic winter, 1992–93, with less PSC, but with an increased burden of aerosols reached 100 ± 25 DU. Interestingly, the difference between column ozone loss in cold Arctic winters

and in the Antarctic winter 2003 is not very large in 380–550 K.

6. Ozone Loss Rates

For calculating ozone loss rates local ozone loss was smoothed over 10 days. Ozone loss rates were estimated by calculating the difference between local ozone loss averaged over the entire vortex core of two following days. as discussed above. Further, the resulting ozone loss rates were again smoothed over ten days, to reduce day-to-day variations. The resulting ozone loss rates (black line) and the corresponding standard deviation (dotted black lines) are shown in Figure 10.

Figure 10.

Ozone loss rates are greatest during mid-September between 380 and 550 K. In 380–420 K ozone loss rates indicate a small maximum during mid-August of ≈ 35 ± 10 ppbv per day and, further, a strong increase until mid-September up to 58 ± 15 ppbv per day. At the beginning of October, ozone loss rates are nearly zero at 380–420 K, because no ozone is left that could be destroyed.

At 430–470 K, ozone loss rates are similar to those at 380–420 K. However, slightly smaller ozone loss rates are deduced for the end of August compared to some weeks before, that may be caused by strongly decreasing A_{PSC}. In correspondence the mean cloud top height detected by MIPAS is below 450 K at this time. With increasing solar illumination, ozone loss rates are increasing as well up to 82 ± 10 ppbv per day. The occurrence of PSC events detected by MIPAS at mid-September in these altitudes may further enhance ozone loss rates (Figure 2). As in 380–420 K, ozone loss rates are nearly zero at the beginning of October when ozone is almost completely destroyed.

At 520–560 K, during July and August, ozone loss rates are more variable and smaller compared to altitudes below, in correspondence with smaller a A_{PSC} and the resulting less chlorine activation. However, a strong increase of ozone loss rates of up to 90 ± 15 ppbv per day at September 24, occurred at mid-September. These ozone loss rates are the strongest that are reported in this study. As discussed in detail in Section 5.2, the history of observed air masses has changed between

September 24–27, 2003. Therefore, we do not interpret these numbers. At altitudes below, this effect seems to be less significant, because strongest ozone loss rates were derived before September, 24, however this potential problem for all altitudes should be kept in mind when comparing these results with other studies.

At 580–620 K the result of tracer-tracer correlations indicate very low ozone loss rates until September 2003. At the beginning of September ozone loss rates of 20 $\pm$ 5 ppbv per day and since mid-September $\approx$ 25 $\pm$ 5 ppbv per day were deduced. This is in correspondence with very little chlorine activation.

7. Comparison with Box Model Simulations

Ozone loss rates derived using tracer-tracer correlations (see Section 6) depend on the time and altitudes considered. Especially during September 10 to 30, 2003, a strong increase of ozone loss rates occurs within the altitude range of 380–560 K.

Box model simulations with the Chemical Lagrangian Model of the Stratosphere (CLaMS) [*McKenna et al.*, 2002b, a] were performed to investigate chemical ozone loss occurring during September 10 to 30, 2003. The box model includes all chemical reactions of stratospheric relevance.

Starting at three isentropic levels, 450, 500 and 550 K, two example vortex air parcel trajectories per level were chosen in a way that the average latitude of the trajectories is about 80°S with the standard deviation of the latitude is smallest and largest, respectively. Therefore, the one example trajectories stays close to 80°S whereas the other show excursions to lower latitude regions. Along these trajectories chemical ozone loss is simulated by the CLaMS chemistry module, whereby the initialization is compiled from ILAS-II data for equivalent latitudes poleward 75°S. Further, total inorganic chlorine was derived from a relations with CH_4 [*Grooß et al.*, 2002] and total inorganic nitrogen from a correlation with N_2O [*Grooß et al.*, 2004]. Total inorganic bromine was set to 22 pptv. These simulations were performed to investigate in how far the observed ozone depletion rate can be reproduced.

The simulated ozone mixing ratios and the corresponding ILAS-II observations are shown in Figure 11. As explained above, on a specific day, observed ozone mixing ratios are varying due to the different history of the observed air masses. However the general amount of ozone depletion is well reproduced be the simulations between September 10–30, 2003, for the three considered theta levels (Figure 11). The simulations show that the large ozone loss rates are a result of long sunlight time and still low temperatures causing very efficient chlorine catalyzed ozone loss.

Figure 11.

Between September 24 and 26, 2003, the large variations of ozone mixing ratios are a result of changing history of airmasses (Section 5.2) and are not caused by chemical effects. This effect seems to be most significant at latitudes above 500 K. However, the model simulated ozone loss rates of $\approx$ 65 ppbv/day at 450 K between September 10 and 30,, that is in well agreement with ILAS-II results at 430–470 K (Figure 10, second panel). The results are also in general agreement with model simulations of the Antarctic ozone hole by *Brasseur et al.* [1997]. In that study, ozone loss rates of 80 ppbv per day were derived during September.

Further, the simulated NO_2 and $ClONO_2$ mixing ratios (not shown) are in general agreement with the – not yet validated – ILAS-II measurements. As for ozone, variations of the mixing ratios of NO_2 and $ClONO_2$ owing to the different history of air masses inside the vortex, as described in Section 5.2, are not represented in box model results.

8. Conclusions

Chemical ozone loss was derived using tracer-tracer correlations based on ILAS-II observations over the entire Antarctic winter 2003. We consider ozone loss inside the polar vortex core only. The edge of the polar vortex was defined according to the *Nash et al.* [1996] criterion; meteorological analysis were taken from UKMO.

During August, accumulated ozone loss of 0.79 ppmv between 400 and 550 K

was derived. During September, the local ozone loss averaged between 400 and 550 K significantly increases up to 2.3 ppmv ozone loss. Between 380 and 470 K almost the total amount of ozone was destroyed. Ozone mixing ratios indicate a strong inhomogeneity, with day-to-day variations larger than 1 ppmv during the first half of September. Backward trajectory calculations have shown, that these variations are a result of a different history of the observed airmasses, that is in particular, a strong variation of the amount of sunlight time that the air parcel has received before the measurement time. In October, local ozone loss became very homogeneous and reached 2.5 ppmv between 400 and 550 K with a standard deviation of 0.08 ppmv.

The temporal evolution of local ozone loss and accumulated loss in column ozone during July and the end of September are in step with increasing solar illumination on activated air masses. Half of the accumulated loss in column ozone over the winter (157 DU in 350–600 K) occurs during September, 2003. About 88% of the proxy ozone was destroyed within this altitude range.

In the present study it is shown, that accumulated ozone loss and ozone loss rates are strongly dependent on the altitude considered. Although the A_{PSC} is largest at altitudes between 380 and 420 K, accumulated local ozone loss does not exceed 2.3 $\pm$ 0.2 ppmv until September 22–23, 2003, because all the ozone was already destroyed within this altitude interval. At 430–470 K 2.8 $\pm$ 0.2 ppmv ozone were destroyed until October, 2003. At altitudes above, less ozone loss occurred (1.9 $\pm$ 0.2 ppmv in 520–560 K and only 0.4 $\pm$ 0.2 ppmv in 580–620 K).

Ozone loss rates in 380–420 K have a maximum around September 18, 2003, of 58 $\pm$ 15 ppb per day. In 430–470 K 82 $\pm$ 10 ppbv per day were reached around September 19, 2003. Since ozone mixing ratios approach zero, ozone loss rates will decrease. At 520–560 K and 580–620 K ozone loss is much less compared to altitudes below and ozone was not destroyed completely, this is in correspondence with smaller A_{PSC} and therefore possible less strong chlorine activation.

Box model results using the CLaMS model reproduce the general temporal

development of ozone mixing ratios between September 10 to 30, 2003. It is shown, that large ozone loss rates at the second half of September are a result of halogen catalyzed destruction enhanced by the strong increase of solar illumination of the vortex area during this time of the year.

The evolution of ozone loss derived in this study is further of interest considering the previous Antarctic winter 2002. In 2002, a major warming occurred at 21 September 2003 [*Newman and Nash*, 2004] and ozone loss came to a halt [*Hoppel et al.*, 2003]. Ozone depletions rates in the polar vortex region rapidly decrease to zero [*Grooß et al.*, 2005]. If such an event would have happened in winter 2003, 82% of the entire loss in column ozone in 350–600 K would have been reached. In 380–420 K most of the ozone was already destroyed by September 21, 2003.

Acknowledgments. We acknowledge all members of the science team of the Improved Limb Atmospheric Spectrometer (ILAS-II) led by Dr. Y. Sasano and Dr. H. Nakajima for processing ILAS-II Version 1.4 data. ILAS-II was developed by the Ministry of the Environment, Japan (MOE) and was onboard the ADEOS-II satellite launched by the Japan Aerospace Exploration Agency (JAXA). ILAS-II data were processed at the ILAS-II Data Handling Facility, National Institute for Environmental Studies (NIES). Thanks to European Space Agency for providing MIPAS near-real-time level 1b data and the UK Meteorological Office for providing meteorological analyses.

References

Becker, G., R. Müller, D. S. McKenna, M. Rex, and K. S. Carslaw, Ozone loss rates in the Arctic stratosphere in the winter 1991/92: Model calculations compared with Match results, *Geophys. Res. Lett.*, *25*(23), 4325–4328, 1998.

Becker, G., R. Müller, D. S. McKenna, M. Rex, K. S. Carslaw, and H. Oelhaf, Ozone loss rates in the Arctic stratosphere in the winter 1994/1995: Model simulations underestimate results of the Match analysis, *J. Geophys. Res.*, *105*, 15175–15184, 2000.

Brasseur, G. P., X. Tie, J. Rash, and F. Lefevre, A three-dimensional simulation of the antarctic ozone hole: Impact of anthropogenic chlorine on the lower stratosphere and upper troposphere, *J. Geophys. Res.*, *102*, 8909–8930, 1997.

Chipperfield, M. P., D. K. Weisenstein, L. J. Kovalenko, C. E. Sioris, P. O. Wennberg, K. Chance, M. K. W. Ko, and C. A. McLinden, Sensitivity of ozone to bromine in the lower stratosphere, *Geophys. Res. Lett.*, *32*, Lo5811, 2005.

Ejiri, M. K., et al., Validation of ILAS-II V1.4 nitrous oxide and methane profiles, *J. Geophys. Res.*, 2005, in preparation.

Farman, J. C., B. G. Gardiner, and J. D. Shanklin, Large losses of total ozone in Antarctica reveal seasonal ClO_x/NO_x interaction, *Nature*, *315*, 207–210, 1985.

Goutail, F., J.-P. Pommereau, and F. Lefèvre, Total ozone reduction in the Arctic during the winters 2001 and 2002 from the saoz network and comparison to previous winters, in *Proc. 6th Europ. Symp., EU Air Pollution Res. Rep. 79, Göteborg (Sweden) 2002*, edited by N. R. P. Harris, G. T. Amanatidis, and J. G. Levine, pp. 181–184, 2003.

Grooß, J.-U., G. Günther, R. Müller, P. Konopka, S. Bausch, H. Schlager, C. Voigt, C. M. Volk, and G. C. Toon, Simulation of denitrification and ozone loss for the Arctic winter 2002/2003, *Atmos. Chem. Phys. Discuss.*, *4*, 8069–8101, 2004.

Grooß, J.-U., P. Konopka, and R. Müller, Ozone chemistry during the 2002 Antarctic vortex split, *J. Atmos. Sci.*, *62*, 3, 860–870, 2005.

Grooß, J.-U., et al., Simulation of ozone depletion in spring 2000 with the Chemical

Lagrangian Model of the Stratosphere (CLaMS), *J. Geophys. Res.*, *107*, 8295, 2002.

Harris, J. M., S. T. Oltmans, G. E. Bodeker, R. Stolarski, R. D. Evans, and D. M. Quincy, Long-term variations in total ozone derived from Dobson and satellite data, *Atmos. Envrion.*, *37*, 3167–3175, 2003.

Harris, N. R., M. Rex, F. Goutail, B. M. Knudsen, G. L. Manney, R. Müller, and P. von der Gathen, Comparison of empirically derived ozone loss rates in the Arctic vortex, *J. Geophys. Res.*, *107*(D20), 2002.

Hoppel, K., R. Bevilacqua, D. Allen, G. Nedoluha, and C. Randall, POAM III Observations of the anomalous 2002 Antarctic ozone hole, *Geophys. Res. Lett.*, *30*(7), 2003.

Manney, G. L., L. Froidevaux, M. L. Santee, N. J. Livesey, J. L. Sabutis, and J. W. Waters, Variability of ozone loss during Arctic winter (1991 to 2000) estimated from UARS Microwave Limb Sounder measurements, *J. Geophys. Res.*, *108*, 2003.

McElroy, M. B., R. J. Salawitch, S. C. Wofsy, and J. A. Logan, Antarctic ozone: Reductions due to synergistic interactions of chlorine and bromine, *Nature*, *321*, 759–762, 1986.

McKenna, D. S., J.-U. Grooß, G. Günther, P. Konopka, R. Müller, G. Carver, and Y. Sasano, A new Chemical Lagrangian Model of the Stratosphere (CLaMS): Part II Formulation of chemistry-scheme and initialisation, *J. Geophys. Res.*, *107*(D15), 4256, 2002a.

McKenna, D. S., P. Konopka, J.-U. Grooß, G. Günther, R. Müller, R. Spang, D. Offermann, and Y. Orsolini, A new Chemical Lagrangian Model of the Stratosphere (CLaMS): Part I Formulation of advection and mixing, *J. Geophys. Res.*, *107*(D16), 4309, 2002b.

Molina, L. T., and M. J. Molina, Production of Cl_2O_2 from the selfreaction of the ClO radical, *J Phys Chem*, *91*, 433–436, 1987.

Müller, R., P. J. Crutzen, J.-U. Grooß, C. Brühl, J. M. Russel III, and A. F. Tuck, Chlorine activation and ozone depletion in the Arctic vortex: Observations by the

Halogen Occultation Experiment on the Upper Atmosphere Research Satellite, *J. Geophys. Res.*, *101*, 12531–12554, 1996.

Müller, R., J.-U. Grooß, D. S. McKenna, P. J. Crutzen, C. Brühl, J. M. Russell, L. L. Gordley, J. P. Burrows, and A. F. Tuck, Chemical ozone loss in the Arctic vortex in the winter 1995-1996: HALOE measurements in conjunction with other observations, *Ann. Geophys.*, *17*, 101–114, 1999.

Müller, R., U. Schmidt, A. Engel, D. S. McKenna, and M. H. Proffitt, The O_3/N_2O relationship from balloon-borne observations as a measure of Arctic ozone loss in 1991-1992, *Q. J. R. Meteorol. Soc.*, *127*, 1389–1412, 2001.

Müller, R., S. Tilmes, P. Konopka, and J.-U. Grooß, Change of ozone/tracer relations in the polar vortex due to mixing and chemistry, *Atmos. Chem. Phys. Discuss.*, *in preparation*, 2005.

Nakajima, H., et al., Characteristics and performance of the Improved Limb Atmospheric Spectrometer-II (ILAS-II) onboard the ADEOS-II satellite, *J. Geophys. Res.*, 2005, in preparation.

Nash, E. R., P. A. Newman, J. E. Rosenfield, and M. R. Schoeberl, An objective determination of the polar vortex using Ertel's potential vorticity, *J. Geophys. Res.*, *101*, 9471–9478, 1996.

Newman, P., and E. Nash, The unusual southern hemisphere stratosphere winter of 2002, *J. Atmos. Sci.*, 2004, in press.

Proffitt, M. H., J. J. Margitan, K. K. Kelly, M. Loewenstein, J. R. Podolske, and K. R. Chan, Ozone loss in the Arctic polar vortex inferred from high altitude aircraft measurements, *Nature*, *347*, 31–36, 1990.

Rex, M., R. J. Salawitch, M. L. Santee, J. W. Waters, K. Hoppel, and R. Bevilacqua, On the unexplained stratospheric ozone losses during cold Arctic Januaries, *Geophys. Res. Lett.*, *30*(1), 2003.

Rex, M., R. J. Salawitch, P. von der Gathen, N. R. Harris, M. P. Chipperfield, and B. Naujokat, Arctic ozone loss and climate change, *Geophys. Res. Lett.*, *31*, 2004.

Rex, M., et al., Chemical depletion of Arctic ozone in winter 1999/2000, *J. Geophys. Res.*, *107*, 2002.

Salawitch, R. J., et al., Chemical loss of ozone during the Arctic winter of 1999-2000: an analysis based on balloon-borne observations, *J. Geophys. Res.*, *107*, 8269, doi:10.1029/2001JD000620, 2002.

Solomon, S., R. R. Garcia, F. S. Rowland, and D. J. Wuebbles, On the depletion of Antarctic ozone, *Nature*, *321*, 755–758, 1986.

Spang, R., J. J. Remedios, S. Tilmes, and M. Riese, MIPAS observation of polar stratospheric clouds in the Arctic 2002/3 and Antarctic 2003 winters, *Adv. Space. Res.*, p. accepted, 2005.

Tilmes, S., R. Müller, J.-U. Grooß, D. S. McKenna, J. M. Russell, and Y. Sasano, Calculation of chemical ozone loss in the Arctic winter 1996-1997 using ozone-tracer correlations: Comparison of Improved Limb Atmospheric Spectrometer (ILAS) and Halogen Occultation Experiment (HALOE) results, *J. Geophys. Res.*, *108*, 4045, 2003.

Tilmes, S., R. Müller, J.-U. Grooß, and J. M. Russell, Ozone loss and chlorine activation in the Arctic winters 1991–2003 derived with the tracer-tracer correlations, *Atmos. Chem. Phys.*, *4*(8), 2181–2213, 2004.

Tilmes, S., R. Müller, A. Engel, and J. M. Russell, Chemical ozone loss: Arctic and Antarctic in comparison, *Geophys. Res. Lett.*, *in preparation*, 2005a.

Tilmes, S., R. Müller, J.-U. Grooß, H. Nakajima, and Y. Sasano, Development of tracer relations and chemical ozone loss during the setup phase of the polar vortex, *J. Geophys. Res.*, *to be submitted*, 2005b.

Urban, J., et al., Odin/SMR limb observations of stratospheric trace gases: Validation of NO2, *jgr*, *110*, D09301, doi:10.1029/2004JD005394, 2005.

S. Tilmes, R. Müller, J.-U. Grooß, Forschungszentrum Jülich, ICG-I, 52425 Jülich, Germany (e-mail: Simone.Tilmes@t-online.de,tilmes@ucar.edu).

Received _____

Figure Captions

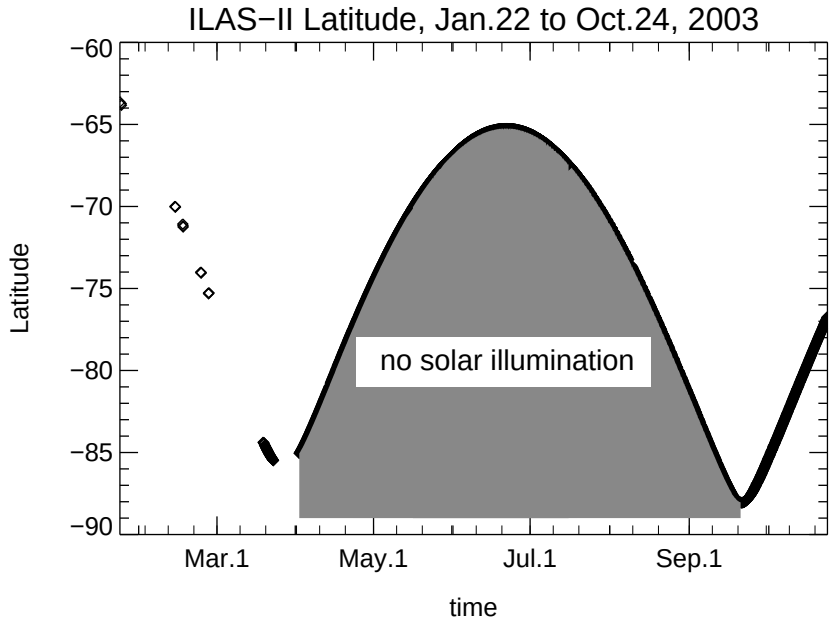

Figure 1. Temporal and spatial coverage of ILAS-II observations in southern latitudes from January 22 to October 24, 2003. The dark area shows the location were the solar zenith angle is less than 90^o.

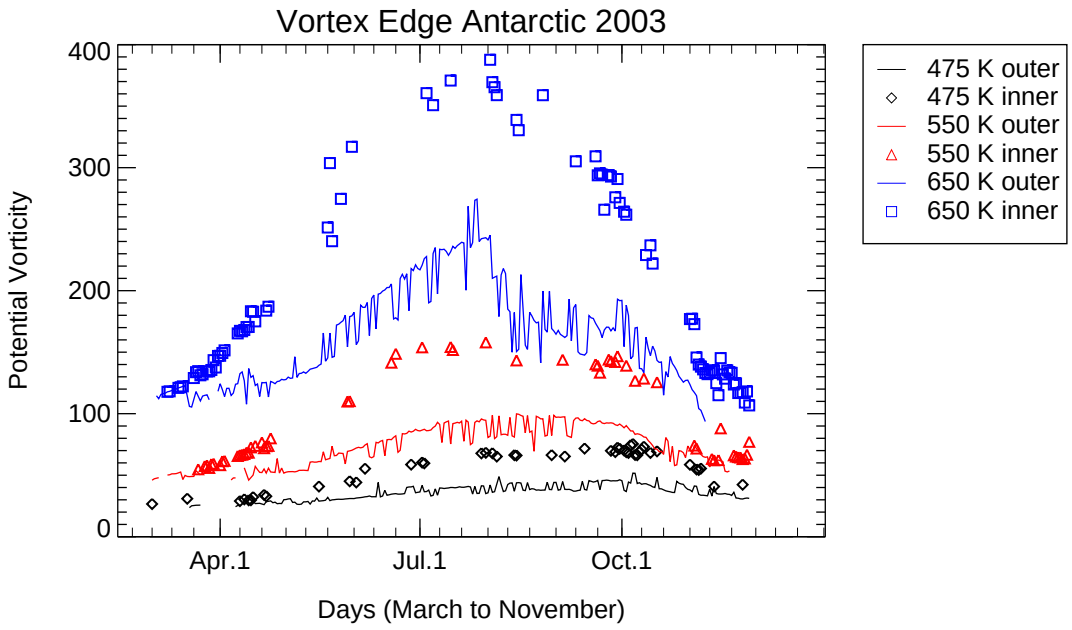

Figure 2. Potential vorticity at the edge of the inner vortex, calculated within the region poleward of 70°S equivalent latitude (colored symbols), and at the edge of the outer vortex calculated within equivalent latitudes equatorward of 70°S (colored lines), during March to November 2003. Different colors show different levels: 475 K, 550 K and 650 K,

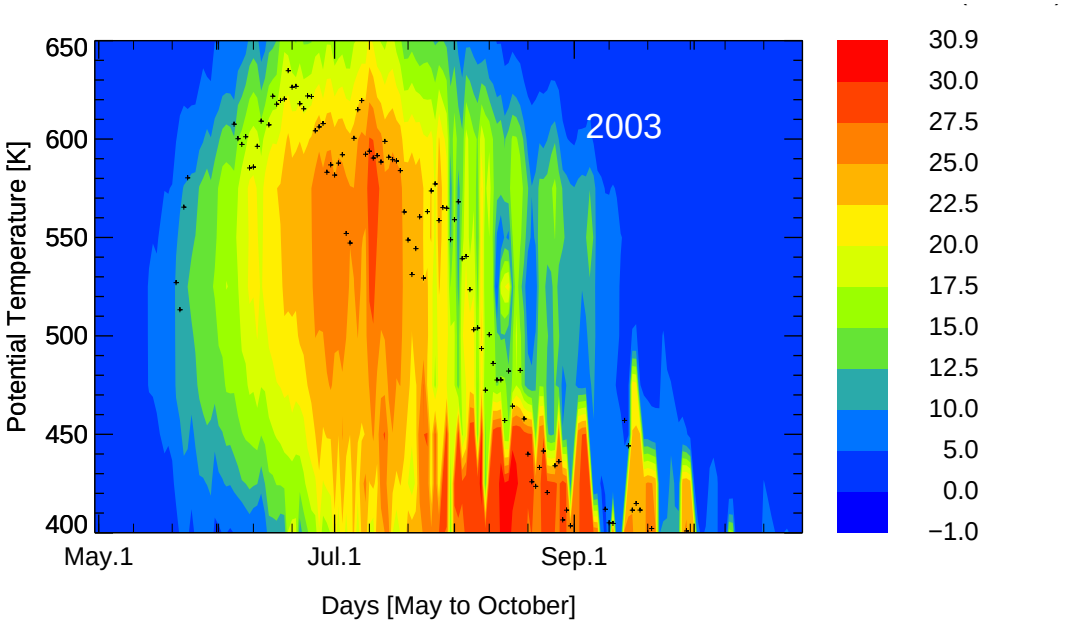

Figure 3. The area of possible PSC existence in 10^6 km^2 over the entire polar vortex, as a function of altitude, is shown for the time period from May to October 2003. The PSC threshold temperature was calculated with the analyzed UKMO temperatures and pressures together with averaged mixing ratios of ILAS-II HNO_3 and H_2O measurements at the corresponding time and altitude. Daily mean cloud top heights of PSC events detected by MIPAS/ENVISAT are shown as black plus signs.

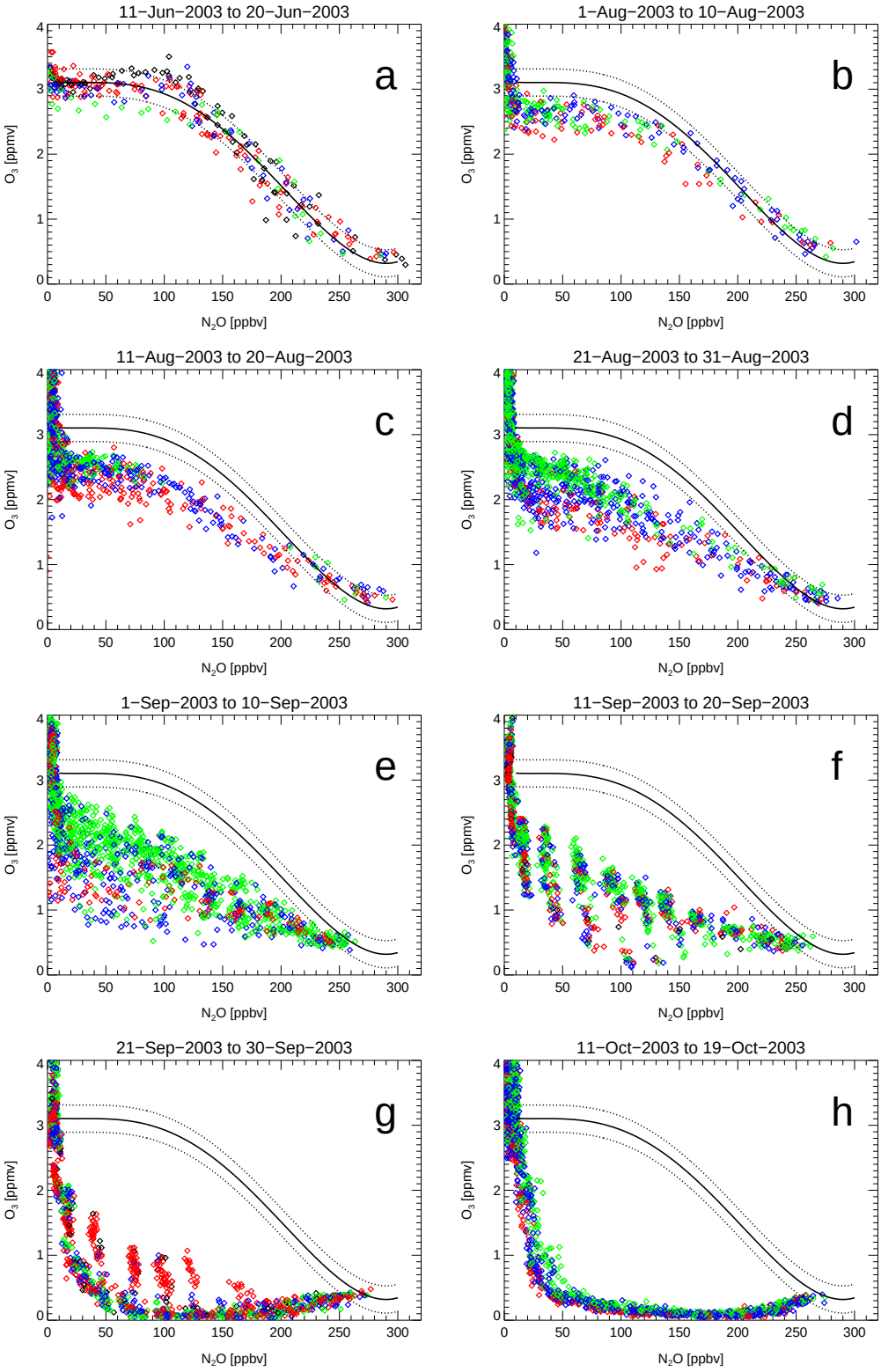

Figure 4. O_3/N_2O relation inside the Antarctic vortex core 2003 during June to October 2003, form ILAS-II measurements derived using the *Nash et al.* [1996] criterion. Black line is the early winter reference function derived for June 11–20, 2003 (panel a) with the area of uncertainty (dotted lines). Different colors indicate different range of equivalent latitude of vortex profiles: 65–70°S (black), 70–75°S (red), 75–80°S (blue), 80–90°S (green).

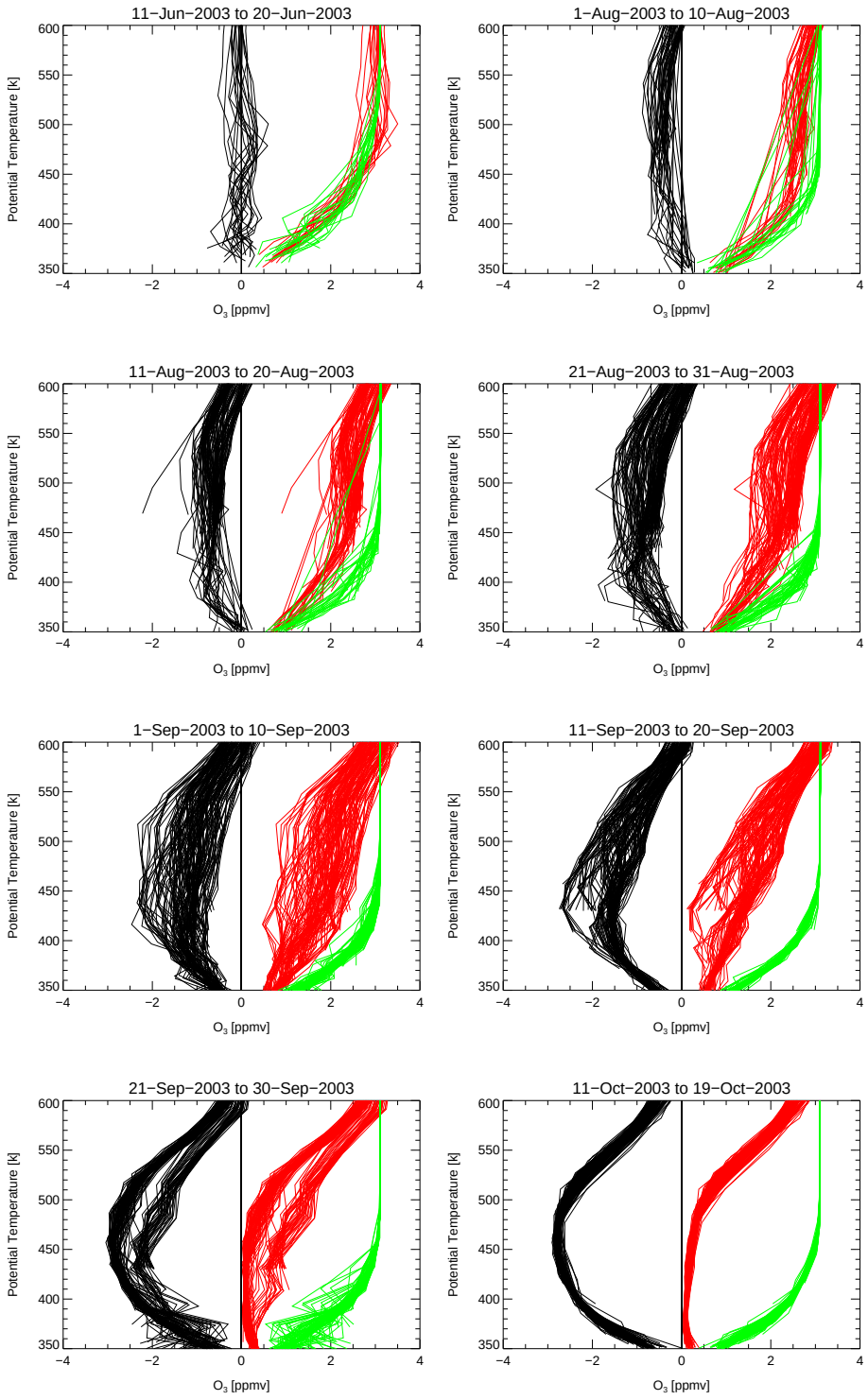

Figure 5. Vertical profiles (plotted against potential temperature) of ozone mixing ratios (red lines) by ILAS-II. The mixing ratios expected in the absence of chemical change (green lines), and the difference between expected and observed mixing ratio of ozone (black lines) are shown for profiles located inside the vortex core using the *Nash et al.* [1996] criterion. The green lines were inferred using N_2O as the long-lived tracer and the early winter reference functions Equations 1. derived in June 11–20.

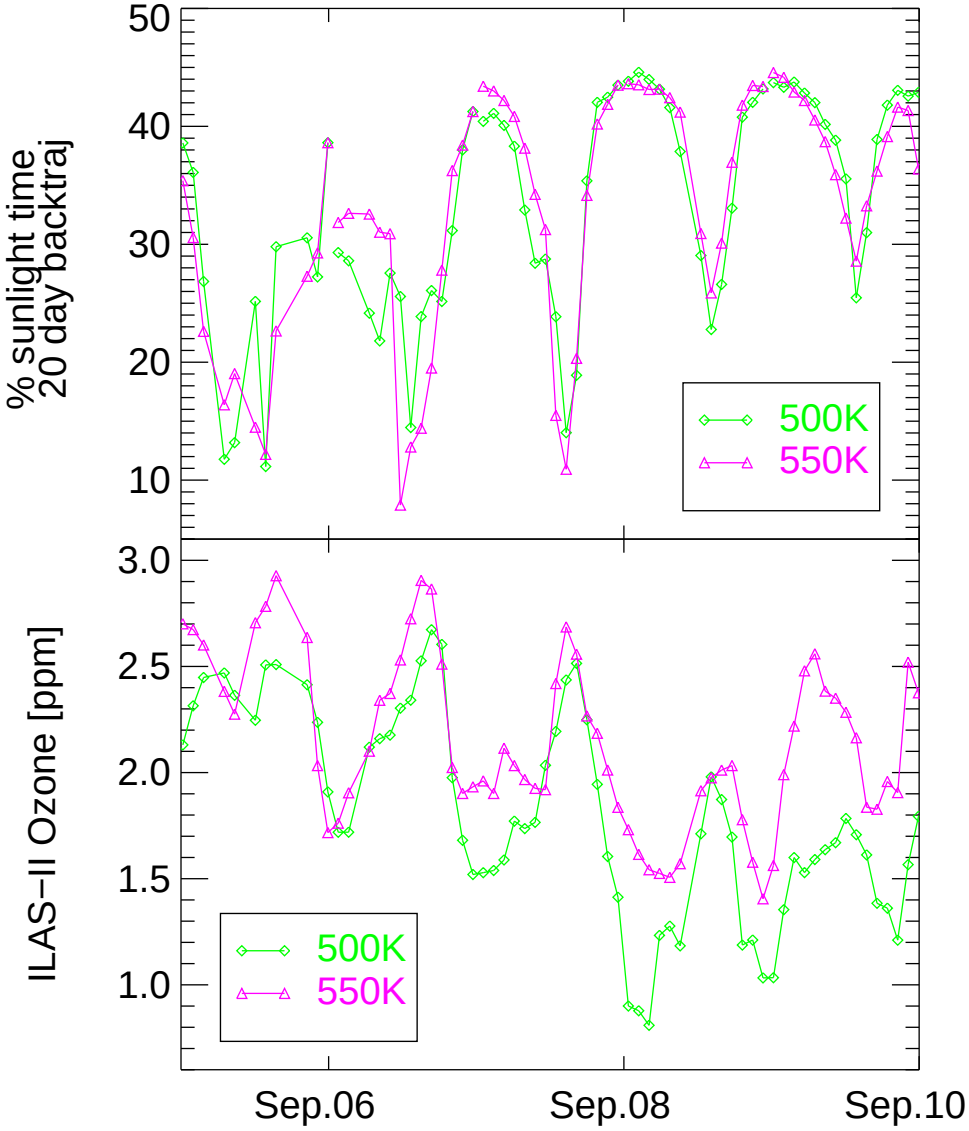

Figure 6. Sunlight time for 20 day backward trajectory calculations of ILAS-II measurements inside the vortex core (top panel), September 5-10, 2003. ILAS-II ozone mixing ratios inside the vortex core (bottom panel).

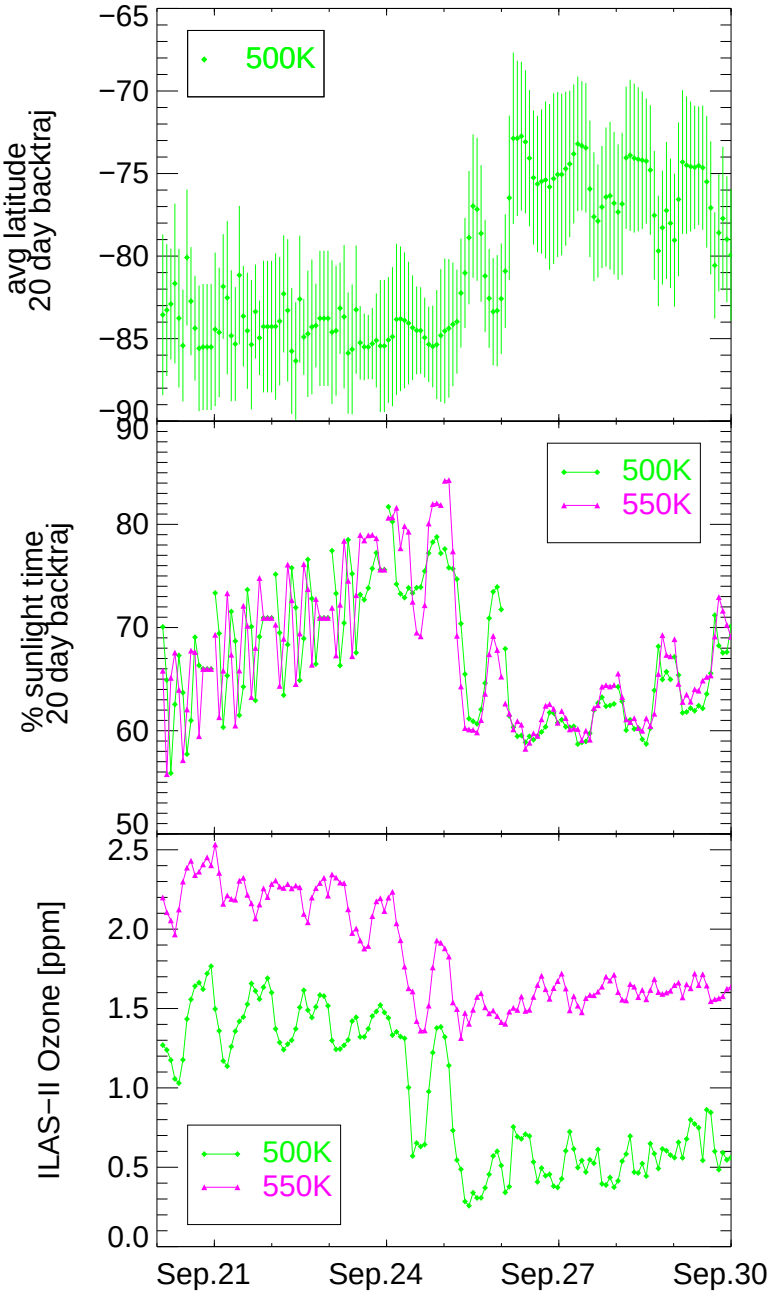

Figure 7. Averaged latitude (top panel, sunlight time (middle panel) and ozone mixing ratios (bottom panel)for 20 day backward trajectory calculations of ILAS-II measurements inside the vortex core, September 21-30, 2003.

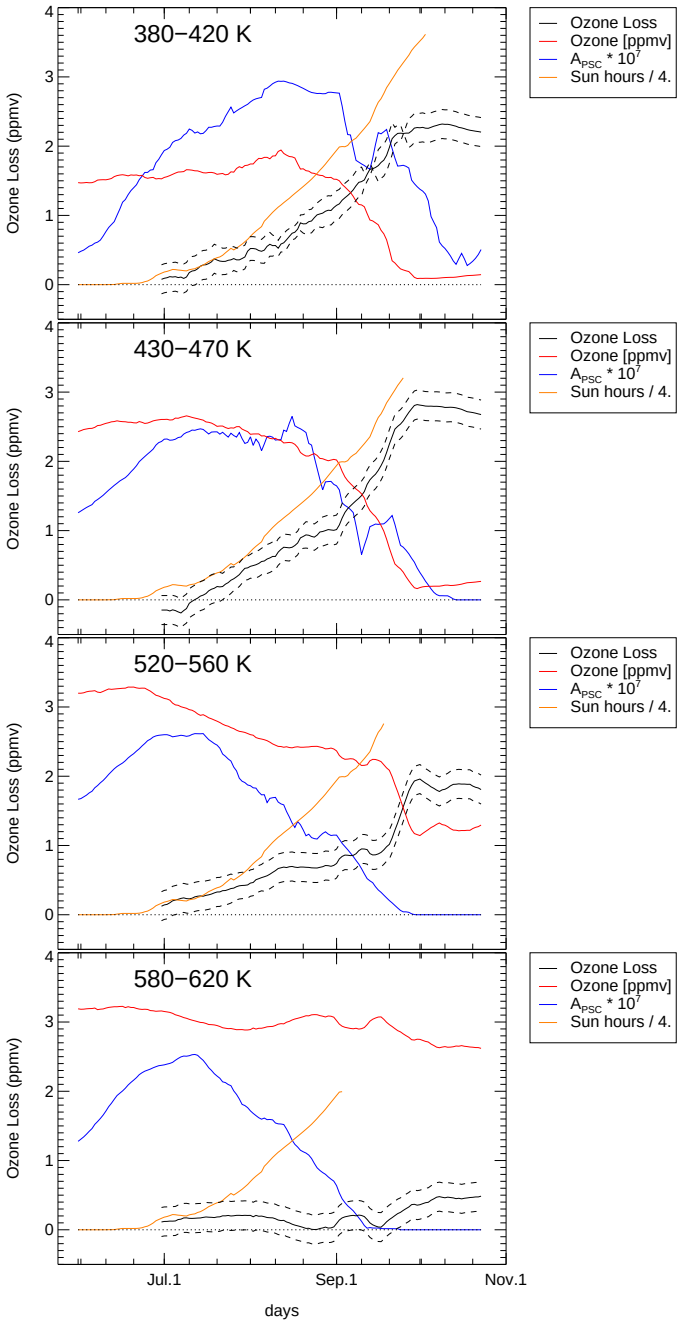

Figure 8. Temporal evolution of local accumulated chemical ozone loss in ppmv in the vortex core, between July and October 2003, for different altitude intervals, smoothed over 10 days. Further shown is the uncertainty of ozone loss (black dashed line), Area of possible PSC existence (blue line), Sun hours per day on the possible PSC area and measured ozone mixing ratios.

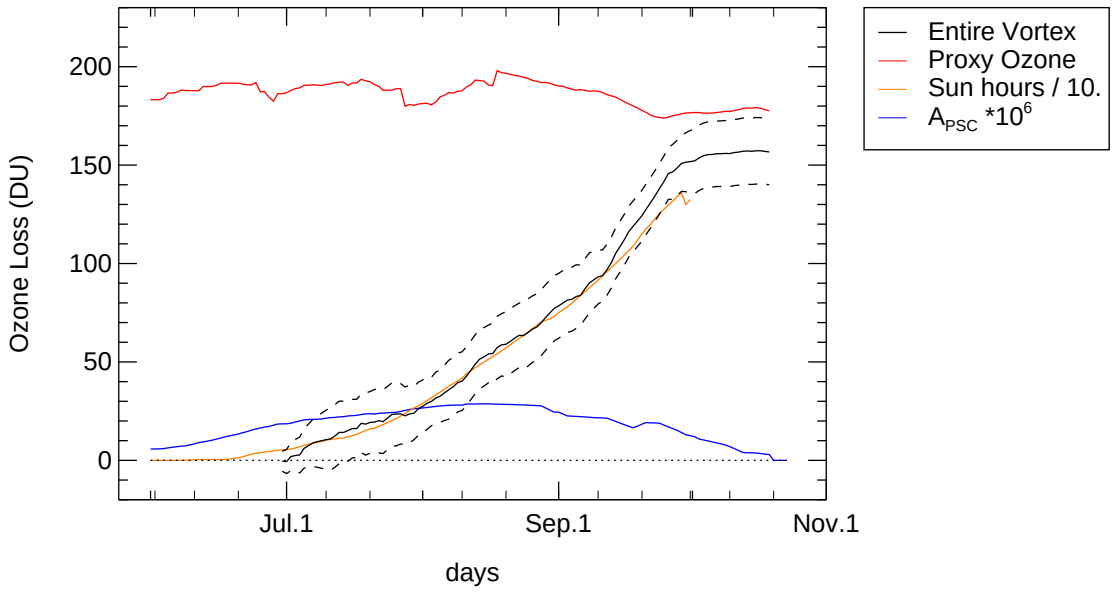

Figure 9. Temporal evolution of accumulated chemical loss in column ozone in 350–600 K inside the vortex core, between July and October 2003 (black line), smoothed over 20 days, uncertainty of ozone loss (black dashed line), area of possible PSC existence (blue line), proxy ozone for chemical unperturbed conditions (red line).

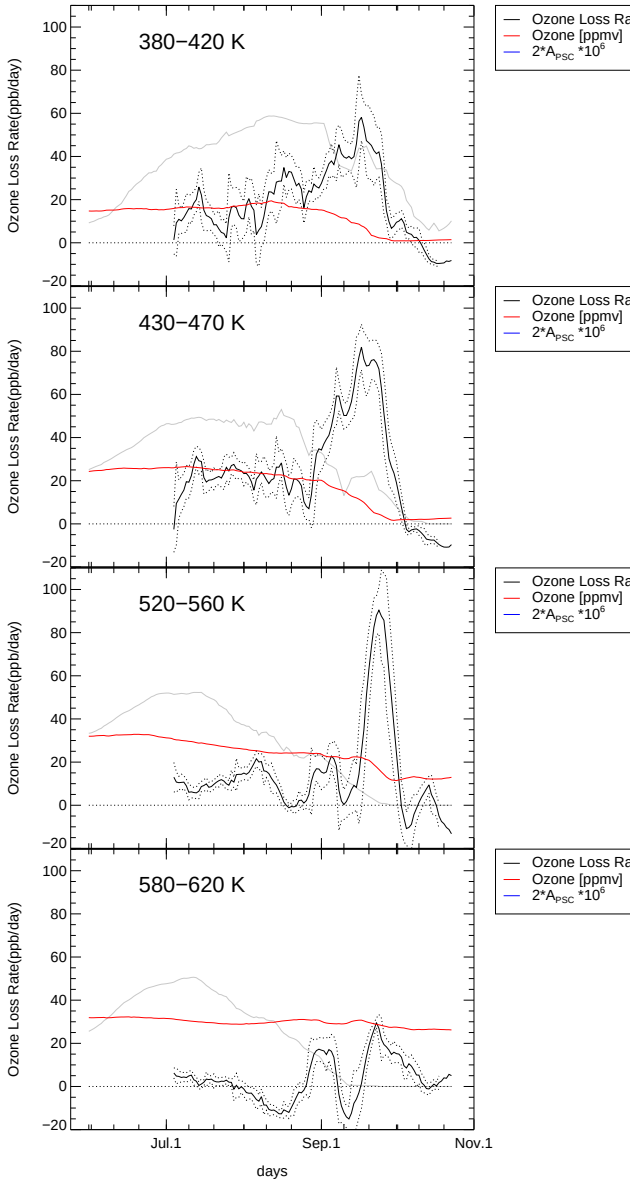

Figure 10. Temporal evolution of local ozone loss rates in ppbv per day averaged over the vortex core, between July and October 2003 (black line), derived from local accumulated chemical ozone loss (as shown in Figure 8), smoothed over 10 days. Dotted lines indicate the uncertainty derived from the standard deviation of ozone loss rates. Further, the volume of possible PSC existence (grey line) and measured ozone mixing ratios (red line) is shown.

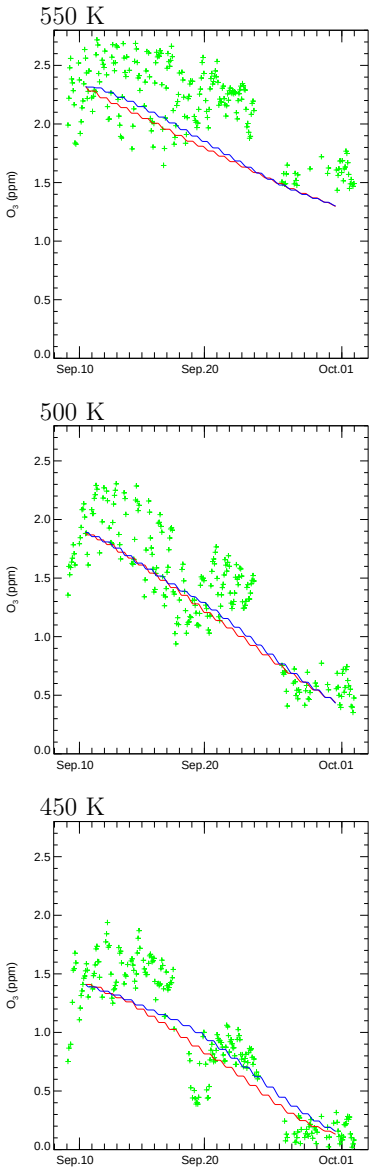

Figure 11. ClaMS box model results for ozone loss in austral spring 2003: equivalent latitude 80 ± 3°S (red line), 80 ± 7°S (blue line). ILAS-II measurements /green symbols) at equivalent latitude > 75°S.